

Frequency analysis of GPS data for structural health monitoring observations

Hüseyin Pehlivan*

Department of Geodetic and Photogrammetric Engineering, Gebze Technical University, Kocaeli, Turkey

(Received September 16, 2017, Revised January 30, 2018, Accepted January 31, 2018)

Abstract. In this study, low- and high-frequency structure behaviors were identified and a systematic analysis procedure was proposed using noisy GPS data from a 165-m-high tower in İstanbul, Turkey. The raw GPS data contained long- and short-periodic position changes and noisy signals at different frequencies. To extract the significant results from this complex dataset, the general structure and components of the GPS signal were modeled and analyzed in the time and frequency domains. Uncontrolled jumps and deviations involving the signal in the time domain were pre-filtered. Then, the signal was converted to the frequency domain after applying low- and high-pass filters, and the frequency and periodic component values were calculated. The spectrum of the tower motion obtained from the filtered GPS data had dominant peaks at a low frequency of 1.15572×10^{-4} Hz and a high frequency of 0.16624 Hz, consistent with two equivalent GPS datasets. Then, the signal was reconstructed using inverse Fourier transform with the dominant low frequency values to obtain filtered and interpretable clean signals. With the proposed sequence, processing of noisy data collected from the GPS receivers mounted very close to the structure is effective in revealing the basic behaviors and features of buildings.

Keywords: noisy GPS data; time series; filtration; fourier transformation; structural monitoring

1. Introduction

Due to its high speed and accuracy in data sampling, Global Positioning System (GPS) is the most common and popular Global Navigation Satellite System (GNSS) technique, with many applications in a wide range of areas. In particular, GPS-recorded data is a unique alternative to continuous monitoring in health monitoring studies; however, it presents with certain challenges (Pehlivan *et al.* 2013). For example, GPS data includes displacements, atmospheric faults, and antenna phase center errors, as well as low-frequency components due to possible multipath errors (Hristopulos *et al.* 2007, Ogaja and Satirapod 2007, Yi *et al.* 2011a). That is, real-time raw GPS sequences contain long- and short-periodic position changes, as well as a mixture of varying noisy signals at different frequencies (Herring *et al.* 2016). Distinguishing and interpreting periodic position changes that represent the movements of the structure in raw GPS data constitute an important problem. To eliminate this problem, researchers have suggested using filters before calculating semi-static and static displacement components from noisy time series (Yan *et al.* 2003, Roberts *et al.* 2004, Gikas 2012, Yi *et al.* 2012, Moschas and Stiros 2013). In this context, effective and sensitive analytical methods are needed to distinguish structural changes and vibrations in noisy datasets (Nickitopoulou *et al.* 2006, Hristopulos *et al.* 2007). For this purpose, in order to calculate the periodic mode values representing the movements of the structure and their amplitudes from GPS, the data recorded in time series

should be examined as a function in time and frequency domains.

Firstly, in the time domain, it is necessary to remove the abnormal and excessively deviated uncontrolled data from the series on the time axis. A general threshold value applied to such signals in the time dimension results in a significant part of the periods falling below the threshold (Elbeltagi *et al.* 2015). Thus, in the time domain, a complete series with a lower standard deviation is obtained before filtering. A low or high pass filter is applied to highlight the low- and high-frequency components and suppress the others, respectively.

Secondly, in the frequency domain, a method known as spectrum analysis is used for a complete and detailed examination of all the periods in the signal. This method refers to time-series analysis in the frequency domain. In a broader sense, the periodic components that occur between observations at different points in time are examined in the frequency dimension. Commonly, in structural health monitoring studies, meaningful periodic components of continuous GPS signals can be determined by switching between Fourier transform (FT) and time-frequency (Welsch 1996). A considerable number of studies have been carried out on the displacement calculation of GPS series using FT (Satirapod *et al.* 2001, Xu *et al.* 2002, Li *et al.* 2006, Erdoğan and Gulal 2009, Yigit *et al.* 2010, Goudarzi *et al.* 2012, Pehlivan *et al.* 2013, Yi *et al.* 2013a, b, Kaloop and Kim 2014, Yigit 2016).

In this study, a systematic approach was adopted to analyze the noisy GPS data obtained from the Endem TV tower located in İstanbul, Turkey. Simultaneous data was collected from two GPS receiver antennas mounted at a height of 165 m at a distance of 1.20 m from the north and south walls of the tower. Due to the proximity of the

*Corresponding author, Ph.D.
E-mail: hpehlivan@gtu.edu.tr

$$y^i = \underbrace{y_0^i}_{\text{observed position}} + \underbrace{v^i(t-t_0)}_{\text{Linear velocity term}} + \underbrace{A_0^i \cos\left(\frac{2\pi(t-t_0)}{\tau_0} - \tau_0\right)}_{\text{Annual period sinusoid}} + \underbrace{A_1^i \cos\left(\frac{2\pi(t-t_0)}{\tau_1} - \tau_1\right)}_{\text{Semi-annual period sinusoid}} + \underbrace{\varepsilon}_{\text{White noise}}$$

Fig. 1 Characteristics and components of the time series (Floyd 2017)

receivers to the tower wall, abnormal noisy data was obtained at certain times of the day as a result of the effect of error sources such as multipath and satellite geometry failure. To analyze noisy data in more detail, the proposed filtering approach was implemented using cyclic codes that linearly advance in the Matlab environment. Using this procedure, it was possible to determine the basic natural frequency from noisy GPS measurements.

Excessive deviations that originated from the receiver or the satellite were removed from all series using a local moving averages criterion (LMAC) filter. Subsequently, a weighted moving average (WMA) filter with an adaptively determined window length based on finite-impulse-response (FIR) was used to separate low frequency components (Han and Rizos 2000; Press *et al.* 1992). The GPS data filtered in the time domain was calculated using fast Fourier transform (FFT) and was decomposed into sub-signals. Thus, periodic and frequent repetition frequencies were determined, regardless of which repetitive signals were included in which frequency component of the raw signal and the type of frequency component. The signal was reconstructed using inverse Fourier transform (IFFT) with the dominant frequency values obtained in the previous step to acquire a filtered and interpretable clean signal. Thus, the positional changes in the sampling interval and the measurement sensitivity were modeled, depending on the time and variables at which the measurement took place. The fundamental frequency values of the tower displacement were obtained from the spectral analysis of the filtered noisy GPS signal. The results were verified with the values calculated from both receivers.

2. Data analysis method

2.1 The determination of displacement amplitude and frequency values

The model of the characteristics and components of the raw GPS time series recorded at fixed intervals in the time domain were taken from Floyd (2017) and are shown in Fig. 1.

The model can be considered as a GPS displacement vector (y) for structural health monitoring. In this case, the initial position and linear velocity term indicate that the displacements of the real dominant frequency, and annual and semiannual sinusoids are considered as low-frequency fluctuations from various sources; e.g., multipaths. White noise corresponds to discontinuous jumps in the signal caused by the receiver and/or satellite outages, cycle slips, etc. (Hristopulos *et al.* 2007). Here, the real displacement

component of interest is suppressed by low-frequency fluctuations and white noise from non-stationary components. The actual displacement has much smaller amplitude than non-stationary components. For this reason, it is possible for low-frequency displacements to be accompanied by low-frequency noise.

The raw GPS signal contains with complex information that can be used to determine meaningful displacement amplitude and frequency values (i.e., sinusoidal components) which reflect the motion of the structure; thus, it should first be examined in the time dimension. Furthermore, the estimation of uncertainties and deviations in the signal is made possible by the precise knowledge of the signal spectrum in order to determine the periodics (dynamic and semi-static displacements) in the signal. The GPS data analysis process recommended consists of the following six stages:

- Analysis in the time domain,
- Low-high pass filtering,
- Signal multiplication with the window function,
- Transformation to the frequency domain and calculation of sinusoids,
- Calculating the power spectrum of the signal,
- Reconstruction of the signal with IFFT.

2.2 Analysis in the time domain

In the first step, abnormal data random errors such as deviations in the series must be eliminated. Since such data occurs in a short period over the entire sequence, the separation of the faulty elements from the GPS series does not significantly affect the statistical properties of the series, but allows performing a more robust spectral analysis.

In the literature, standard deviation values are used as a criterion for the removal of uncontrolled jumps and deviations in raw series. As an alternative to standard deviation, other robust dispersion estimates, such as median absolute deviation and m-estimators can be used instead of the standard deviation (Mertikas 1994). An iterative algorithm has been developed to remove all abnormal outliers. To separate non-normal distribution fluctuations and jumps revealed, the mean extreme deviation criterion (threshold value) is used (Hristopulos *et al.* 2007).

$$|y_{kt} - \tilde{y}_{kt}| = 4\sigma_{kyt} \quad (1)$$

where the standard deviation of y_t is σ_{yt} , with \tilde{y}_t being the average of the samples with m elements, and k represents the iteration order of the filter. \tilde{y}_t is called the LMAC of a y_n series with n elements which are standardized with $y_n = y_t - \tilde{y}_t$ equality. Each $t \in \{t_1, \dots, t_n\}$ element is calculated as follows

$$\tilde{y}_t = \frac{\sum_{t-m}^{t-1} y(t)}{m} \quad (2)$$

where every average value for t time is iteratively calculated with a moving average in a window of $(t-m)$ size. Here, the value of m can be determined by considering the sampling interval of the data. The LMAC values of the series y_t for each t value are calculated using the $(t-m)$ window widths. If the value of y_t is greater than $4\sigma_{kyt}$, the calculated average value is assigned to this data. Otherwise,

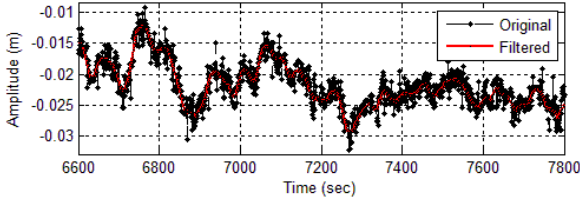


Fig. 2 Noisy data and low-pass filtering

the normal value is maintained in the series, and the removing process for each t is carried out using the following equation;

$$y_t = \begin{cases} \tilde{y}_t & , \quad -|4\sigma_{y_t}^k| > y_t > +|4\sigma_{y_t}^k| \\ y_t & , \quad -|4\sigma_{y_t}^k| < y_t < +|4\sigma_{y_t}^k| \end{cases} \quad (3)$$

With this equation, the y_t series are removed from the uncontrolled data. Thus, extreme deviations from the local average are successfully removed from all series. In addition, the standard deviation criterion can be used as a filtering threshold in LMAC instead of $4\sigma_{y_t}$, depending on the nature of the data used in the study.

2.3 Filtering

In general, although the statistical and systematic characteristics of GPS noise are not fully known, the spectral distribution has been suggested as follows (Han and Rizos 1997):

- (1) Atmospheric noise from 5×10^{-5} to 8×10^{-4} Hz,
- (2) the multipath noise from 8×10^{-4} to 10^{-2} Hz,
- (3) the receiver noise from 8×10^{-4} to 2×10^{-2} Hz,
- (4) the noise from various sources from 0 to 10 Hz.

Accordingly, it was hoped that by removing the non-stationary noise component with low-frequency fluctuations, the stationary component including the real displacement and random noise would be obtained. Different filters were applied to clearly reveal the periodicities that occurred in the long- and short-time intervals (i.e., low- and high-frequency components); moving average as a low-pass filter for the former and a high-pass filter for the latter.

2.3.1 Low-pass filtering

The floating average method known as smoothing operation was used to remove the noise component in the time series to reveal the low-frequency periodicities and the trend component. Most filters that perform softening can be considered to be a low-pass type. Many softening algorithms are available including Additive, Savitzky-Golay, Ramer-Douglas-Peucker, Moving Average, and Kalman filters (Duran and Earleywine 2012).

In this study, as a convenient and simple method to extract static and semi-static displacements of structures, WMA was deemed appropriate based on observations of GPS data (Moschas and Stiros 2013). According to the weight model used in MWA, the effect of previous and subsequent values was weighted during the calculation of each variable. Thus, the potential number of variables that would fall outside the accuracy limits was reduced. The

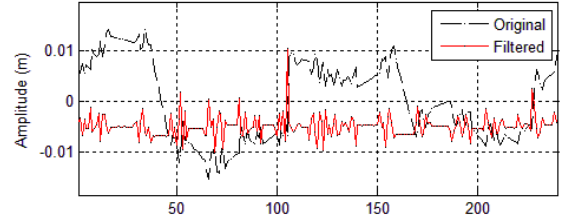


Fig. 3 Noisy data and high-pass filtering

filter applied to a sample signal is shown in Fig. 2. The weight to be assigned was directly related to the window width selected. When a WMA filter with the finite-impulse-response (FIR) structure is applied to a y series with N elements with a window size m , the following equation is used

$$y(k) = \frac{\sum_{k=m+1}^m (y_{k-m} + y_{k-1}) + \sum_{k=m+1}^m (a_{k+1} + a_{k+m})}{2m} \quad (4)$$

2.3.2 High-pass filtering

A differentiation (the successive extractions of serial elements) in a time series is undertaken to clearly reveal the high frequency components (dynamic displacements), and the consecutive differences between the periodic data are calculated (Fig. 3). Thus, the noise components in the consecutive data are partially removed.

The differentiations are carried out by the following equations (Box and Jenkins 1970), with $t=1, 2, \dots, n$ undertaking a differentiation at a 1st degree;

$$\Delta y_{t+1} = y_{t+1} - y_t \quad (5)$$

and carrying out a differentiation at a 2nd degree;

$$\Delta^2 y_{t+2} = y_{t+2} - y_{t+1} = y_{t+2} - 2y_{t+1} + y_t \quad (6)$$

2.4 Window function

In the calculation of the spectrum of a signal with discrete Fourier transformation (DFT), the artificial absence between the last values and the initial values of the signal is thought to be the leakage of energy into other frequencies, which is called spectral leakage. One way to reduce spectral leakage during DFT calculation is the elimination of the absence of the last initial values of the signal. For this purpose, windowing is applied to the signal before DFT (Walker 1996). This method predicts that the signal will be multiplied prior to DFT by a window function that slowly approaches the amplitude towards the edges. In this case, the discontinuity between the final values and the initial values of the signal is reduced. A typical Hamming window function for $w(n)$ with N elements is generally used for this purpose (Press *et al.* 1992, Oppenheim, *et al.* 1999).

$$w(n) = \begin{cases} 0.54 - 0.46 \cos\left(\frac{2\pi n}{N}\right), & 0 \leq n \leq N-1 \\ 0, & n < 0 \text{ ve } n > N-1 \end{cases} \quad (7)$$

2.5 Transformation to the frequency domain and calculation of sinusoids

FT is an indispensable method of analysis in data processing and analysis. In particular, FFT routines are very effective in transforming large data into the frequency domain. The signal was examined in the time domain to determine whether it exhibited periodic properties. FFT was applied for sampling in the frequency domain, depending on the length of the series, and the sampling frequency, amplitude, frequency and phase values were calculated. Using these values, amplitude-frequency and power-frequency graphs were created. All the frequency values contributing to the high-frequency signal to the low frequency can be listed in a frequency-amplitude graph. Thus, all the periodic motions contributing to the signal are determined with the amplitude and frequency values. High-amplitude frequency values are considered as meaningful periodic values in the analysis of GPS data. The low or high frequency peak value of amplitude indicates the magnitude of the periodic motion that occurs. Significant low frequency periodicities occur over long time intervals and are considered to be slow movements. High frequency occurs at short time intervals in meaningful periods and is known as rapid deformations.

For the calculation of frequency values with FT equations for the y signal presented in Fig. 1, the model was further developed as shown in Equation (8) using the series $y(t)$ recorded with GPS receivers over a t time with a specified T sampling interval with the main angular frequency of $\omega = \frac{2\pi}{T} = 2\pi f_0$ in the range of $-\pi \leq \omega T \leq \pi$

$$y(t) = a_0/2 + a_n \cos(\omega n t) + b_n \sin(\omega n t) + c_n t + d_n \delta(t_n) + \dots \quad (8)$$

where $n=0,1,2,\dots$ refers to the harmonic index, a_0 is a constant term, a , b are the Fourier coefficients, c is the long term trend, and d is the possible error values in the series. To clearly reveal the periodic components (a , b coefficients) of the series $y(t)$, the error component (d) must be separated or suppressed using the above-mentioned filtering processes. In addition, the trend component (c) should be removed. After these operations, assuming that the signal length of the intermittent time series $y(t)$ produced by the GPS measurements was equal to the main period, the following equation can be obtained using the Fourier series

$$y(t) = a_0/2 + \sum_{n=1}^{\infty} a_n \cos(\omega n t) + b_n \sin(\omega n t) \\ = a_0/2 + \sum_{n=1}^{\infty} A_n \cos(\omega n t + \phi_n) \quad (8)$$

where A_n is the harmonic amplitude and the phase angle of the ϕ_n Fourier series. FT involves the calculation of frequency values in Eq. (9). When $Y(t)$ is a signal at time t_k ($k=0,1,2,\dots,N-1$) and L is a positive integer, if $N = 2L$, then the periodic component parameters a_0 , a_n and b_n , respectively, would be the coefficients of the real and

imaginary components (Bracewell 2000)

$$a_0 = \frac{1}{N} \sum_{k=0}^{N-1} y(t_k) \\ a_n = \frac{2}{N} \sum_{k=0}^{N-1} y(t_k) \cos(2\pi n k / N) \\ b_n = \frac{2}{N} \sum_{k=0}^{N-1} y(t_k) \sin(2\pi n k / N) \quad (10)$$

where for the number of elements up to $n = 1, 2, \dots, M$, the $N \geq 2M + 1$ condition must be provided. The periodic amplitude and phase angle of the n 'th order element (James 1995) are calculated using the following equations

$$A_n = \sqrt{a_n^2 + b_n^2}, \quad \phi_n = \tan^{-1}(-b_n/a_n) \quad (11)$$

2.5.1 Determination of the frequency values of signal by FT equations

Since GPS signals are discrete signals, the frequency values of an intermittent $y(n)$ time series are calculated by the Discrete Fourier Transform (DFT). The DFT of an intermittent $y(n)$ time series has been described by several researchers (Byrnes *et al.* 1989, Bracewell 2000, Li 2004, Hristopulos 2007)

$$Y(k) = \frac{1}{N} \sum_{n=0}^{N-1} y(n) e^{-j2\pi k n / N}, \quad k = 0, 1, \dots, N-1 \quad (12)$$

Using DFT, the $y(n)$ signal, which is a function of t time, is converted into the frequency domain as the $Y(k)$ signal. The $Y(k)$ signal is a complex number with amplitude and frequency values. The FT algorithm performs N -element series transformation with N^2 complex multiplications and $N \times (N-1)$ additions. The FFT algorithm is used to reduce this transaction intensity and achieve faster conversion (Cooley and Tukey 1965). Even if the serial length is not a multiple of two as required by the Nyquist Theorem, Cooley and Tukey's FFT algorithm can be applied to calculate the value in a short time. The use of FT in the MATLAB environment has greatly reduced the processing load and increased the number of applications for signal processing. Thus, effective calculation algorithms have been developed.

When FFT is applied to GPS measurements, harmonic movements that occur in the frequency domain can be determined, but this does not provide any data on the time these movements take place. For the calculation of the frequency of the signal for each time t , short-time FT must be applied (Li *et al.* 2004).

For analysis in time and frequency dimension, the sampling interval of the signal is important. In a time series recorded with the Δt sampling interval, the sampling frequency is expressed as $f_s = 1/\Delta t$. From this, according to the Nyquist Theorem ($\omega_{Nyq} = \pi/\Delta t$), if a standard FFT is used, these sampling points are located evenly across the frequency range ($[0, \omega_{Nyq}]$). The highest frequency that can be processed is half the sampling frequency ($f_s/2$). The highest calculated frequency is known as the Nyquist frequency. The FT operation periodically determines the number of $N/2$ repetitions in the $-$ and $+$ direction on a signal with N elements. When the frequency sampling range $\Delta f = f_s/N$ is selected, the frequency axis has frequency values as high as $N/2$. N must be multiples of the two, and

Table 1 RTK GPS Measurements Parameters

RTK GPS measurements parameters	Values
Active number of satellites	Minimum: 5
Satellite height	Minimum: 10 degrees
Recording range	20 Hz
Recording date/time	5 days in Dec., 120 hours
Vertical Dilution of Precision	0.9
Cut-off angle	20
Ionospheric models	0.5-2 ppm free model

the data sampling rate must be selected according to the Nyquist sampling theory for avoid a conflict in the frequency spectrum (Blais 1988).

2.6 The power spectral density

To determine the frequencies on which the signal concentrates on, FT is computed by squaring the absolute values of the resulting complex numbers. In this case, the signal's power spectral density (PSD) is defined by the following equation (James 1995)

$$\text{PSD}_m = |Y(k)|^2 \quad (13)$$

In this stage, amplitude-frequency and power-frequency graphs are created and analyzed. The maximum or minimum values of amplitudes indicate the magnitude of the periodic motion that occurs. High amplitude frequency values are considered significant harmonic values in the analysis of GPS data. However, various methods are also used to distinguish meaningful signals from noise, the most common of which are Monte Carlo simulations (Heslop *et al.* 2002).

2.7 IFFT

In this process, the frequency spectrum is used to reconstruct the signal with dominant frequency values from the calculated GPS data. The IFFT operation is performed with the following equation (Bracewell 2000)

$$y(n) = \frac{1}{N} \sum_{k=0}^{N-1} Y(k) e^{j2\pi kn/N} \quad (14)$$

3. Experimental test

A test measurement was performed using a real-time kinematic (RTK) GPS method with dual frequency receivers to determine the structural behavior of a 240 m high television tower (Pehlivan *et al.* 2013, Pehlivan and Bayata 2016). Two rover antennas and receivers were installed at a height of 165 m (Fig. 4) (Yi *et al.* 2011b, c). The GPS base receiver data was continuously transmitted to these two receivers. The position values of both antennas were recorded in a disc with a 20 Hz sampling rate. All the GPS observations was used at the RTK method with a

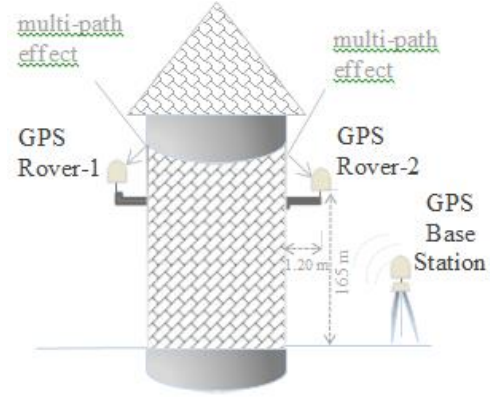


Fig. 4 Locations of tower GPS measuring equipment

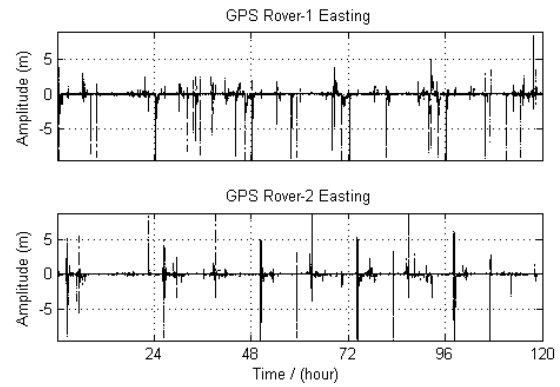


Fig. 5 The five-day records of the original east observation series in R1 and R2

NovAtel GPS OEM4 and using the NovAtel CDU software were recorded into the control unit. RTK GPS measurement parameters are presented in Table 1.

All the data was obtained in the Earth-Centered Earth-Fixed (ECEF) coordinate system and was manually converted to the local topocentric coordinate system for more convenient evaluation. As a result, four datasets (x_1 , y_1 ; x_2 , y_2) for north and east directions were obtained for further analysis. The five-day records of the original raw data series of east (x_1 , x_2) observations in R1 (Rover-1) and R2 (Rover-2) are presented in Fig. 5.

4. Data analysis

Noisy raw signals were obtained due to the inadequate number of satellites, multipaths, etc. These errors probably resulted from the proximity of the rover receivers to the tower walls (up to 120 cm). As shown in Fig. 2, it there was a significant number of excursions outside the range of ± 5 cm. Particularly at certain times of day, it was observed that the - and + direction had significant deviations. Prior to the spectral evaluation of these problematic signals, time dimension analysis and filtering were performed as described in Section 2.

4.1 Analysis in the time domain

First, abnormal values that were not within the specified

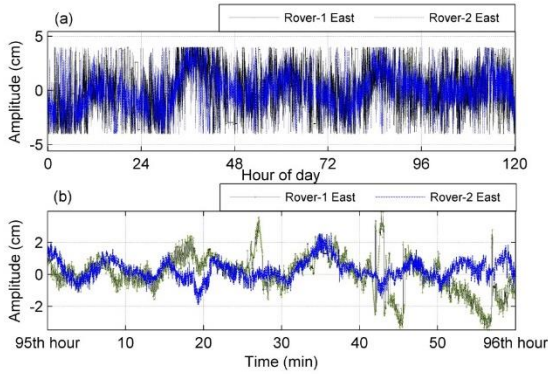


Fig. 6(a) The original and filtered time series for the east GPS signals and (b) zoomed signals between the hours 95 and 96

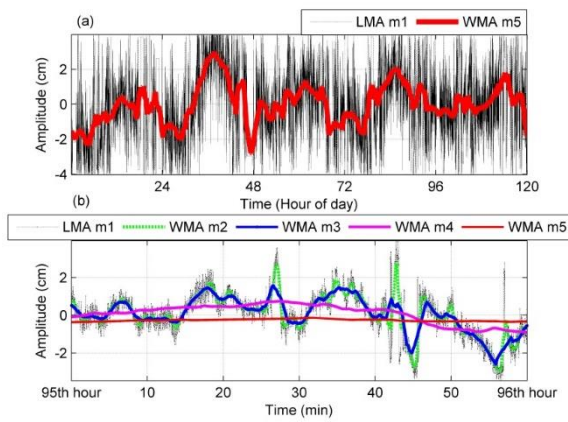


Fig. 7(a) The original and filtered time series for the east GPS signal and b) zoomed signals between the hours 95 and 96

range of values for the structure that was measured were removed from the raw data to obtain better results from the next filtration steps and the spectral analysis. Due to the slow motion of a rigid structure used for this process, standard deviation was assumed to be 1 cm and the threshold value was determined as 4 cm. Using Equation (2) given in Section 2, the values of LMA calculated by taking $m = 2$ (2 min) were assigned as new values for the data outside the lane interval determined by -4 cm and +4 cm. Thus, both the approximate tendency and the number of elements in the series were maintained. After performing this process twice, it was seen that the abnormal values in the dataset had been successfully removed (Fig. 6). Of the four GPS series examined in the following sections, only the east observation series (x_1 , x_2) are shown because the qualitative results were the same for all GPS signals.

4.2 Filtering

The low-frequency noise was removed using a WMA filter. To do this, for each t element on the standardized data, the serial was recalculated with Eq. (3) as described in Section 2, using an “ m ” element window consisting of the previous and next neighbor elements. The width of the “ m ” window used was set to 20, 60, 600 and 3600 seconds. The

series calculated by four different “ m ” values are presented in Fig. 7.

4.3 Signal multiplication with the window function

Test GPS measurements with R1 and R2 receivers were performed continuously with a sampling interval (t) of 0.05 sec at sampling frequency of 20 Hz. Continuously for five days, the number of observations recorded by each receiver was calculated as $N=8.388.608$ (223) and the full duration of the experiment was 116 hours, 30 minutes and 30.4 seconds. ($T = 419.430, 4$ sec). Prior to the spectral analysis, the data vectors were partitioned into $N_{fft}=512$ non-overlapping sections. A linear trend was removed from these sections. A Hamming window (using Equation (7)) was applied to reduce spectral leakage (Oppenheim *et al.* 1999).

5. Spectral analysis

In this section, to determine the periodic components that occurred below 1 Hz (periodic components greater than 1 second) of the structural movement, and for ease of operation, the entire time series were re-sampled at 1-second intervals. Spectral analysis was performed with $218 = 262144$ pieces of data in order to comply with the Nyquist theorem. When applied to the vectors (GPS $x_{1,2}(t)$, $y_{1,2}(t)$), FT in Equation (12) gives information about the number of harmonics that can be obtained by half the number of elements. Accordingly, the harmonic (mod) numbers can be calculated in both series as $\text{mod} = N/2 = 262144/2 = 131072$.

When switching from the time domain to the frequency domain using FFT, the frequency increase is $\Delta f = 1/262144 = 0.000000238418579$ Hz and the data includes the sampling frequency (Δt) for 1 second, $f_{Nyq} = 1/2\Delta t = 0,5$ Hz, which shows the Nyquist frequency, and The frequency resolution of $d_f = \frac{f_c}{N_{fft}} = 9,8$ mHz. The signaling frequency spectra include 131072 periodic mode values ranging from -0.5 Hz to + 0.5 Hz. Here, there are 131072 significant component values between 0 Hz and 0.5 Hz.

5.1 Power spectral density

5.1.1 Low-frequency spectrum

The low-pass filter (WMA) was applied according to Eq. (4) to determine the low-frequency and long-period components from all series. Then, after FFT transformation using Eq. (12), each frequency value, and real and imaginary (bn) coefficients of the series were calculated by Eq. (10). The amplitude and phase angle values corresponding to each frequency value were calculated by Eq. (11) and the power spectrum by Eq. (13).

The standardized form of the signal and its power spectral density are shown in Fig. 8(a) and (b), respectively. Since the spectrum was stationary over 0.0001 Hz, the range of 0.00012 to 0.5 Hz is not shown in the figure. It can be seen that periods with high amplitude concentrated at

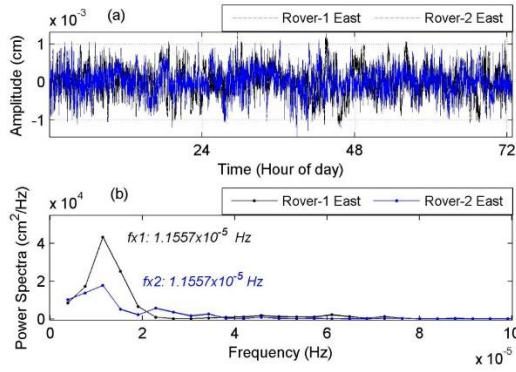


Fig. 8(a) Standardized low-pass filtered signals (x1 and x2) and (b) their PSD

Table 2 Dominant mode values with low frequency calculated from all GPS series

Mode	Computed Frequency (Hz)	Period (Hour)	Amplitude (cm)
First	0.00001157	24	0.6
Second	0.000023	12	0.4
Third	0.000007	36	0.4
fourth	0.000023	72	0.37

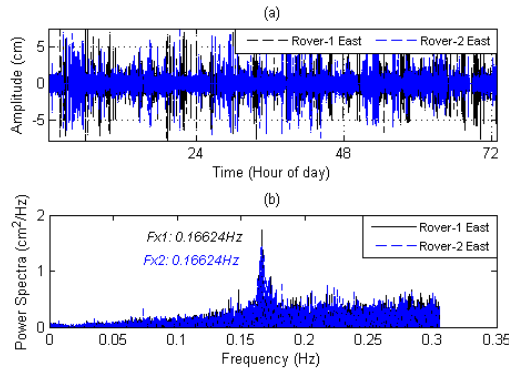


Fig. 9(a) Standardized high-pass filtered x1 and x2 signals and their (b) PSD

low frequency values between 0 Hz and 0.00002 Hz.

In Fig. 8(b), the dominant peak value of x1 and x2 series was 0.0000115572 Hz (fx1, fx2). The peak points and positions in all series were in agreement. The GPS-RTK accuracy was 4 mm (Brownjohn 2005) with the root mean square error (RMS) values of the displacement series being below this value (Fig. 8(a)).

Table 2 presents the common mode values calculated from all GPS series sorted by the amplitude value. The first frequency value with the highest amplitude was the dominant frequency that contributed to the signal. The dominant frequency included the sum of different amplitude signals of the same frequency repeated in the signal.

In R1 and R2 GPS signals, the meaningful periodic components concentrated at low frequencies. The significant and long periodic components of these signals are large-amplitude first mode values (fx1, fx2). Table 2 gives the following information; Mod 1 value: 24 h, Mode 2

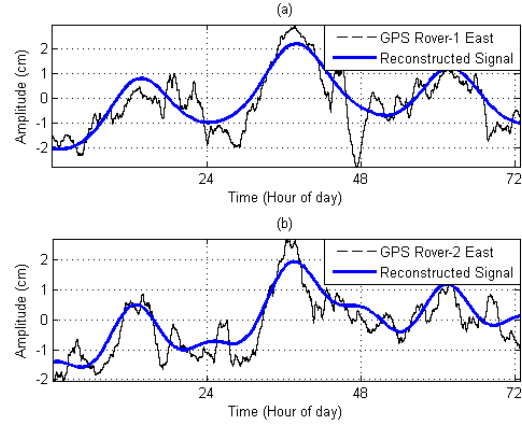


Fig. 10 GPS series reconstructed with dominant frequency values

value: 12 h, Mode 3 value: 36 h, and Mode 4 value: 72 h, which represents the variation in the dominant periodicities. These values indicate the presence of a clear main period that repeats every 24 hours.

5.1.2 High frequency spectrum

Vibration and noise components representing building movements are of high frequency. When a high-pass filter was applied using Eq. (5), it was seen that the frequency of 0.16624 Hz (Fx1, Fx2) was predominant in all series (Fig. 9). This shows that the structure was moving every 6 seconds.

6. Reconstruction of the signal using IFFT

To clearly evaluate the periodic movements of the structure and the change over time, observation orders were reconstructed using IFFT with dominant mode values. During the reconstruction of the GPS signals for the 't' time by Eq. (14) using the dominant mode values given in Table 2, the fluctuations (periodics) in the main signal were modeled and the raw GPS signal was filtered. Fig. 10 shows the variation of the GPS quasi-static and static displacement amplitude over a three-day periods and the apparent ripple of a first mode frequency component every hour.

7. Conclusions

GPS receivers may have to be installed in locations where the sky is not easily visible or is obstructed by the architectural design of some structures and other physical obstacles. In these situations, the data obtained can be noisy and unstable due to error factors in the multipath, satellite geometry and visibility because of the proximity of the receivers to the structure. In this article, the data recorded by two receivers, mounted at a 165 m height and at a proximity of 1.20 m to the tower wall, was examined. An analysis procedure was proposed to determine the structural modes with the test GPS observations and the results of the current study were found to be consistent with those of

previous studies (Hyristopoulos 2007, Pehlivan 2013).

The results and suggestions obtained from this study are as follows:

The raw GPS datasets were found to contain abnormal data varying in time ranging from 1 min to 1.5 h and varying in amplitude from 10 cm to 70 m (Fig. 5). It was estimated that this data may have resulted from the proximity of the receivers to the structure, as well as other random sources of error. For these reasons, a sequence of analyses was required to determine the displacement values from the acquired data required. For this purpose, an analysis process involving six steps was proposed. In the first step, the abnormal data due to jumps and breaks in the GPS observation series was extracted from the dataset to perform a spectral analysis. For this process, a Matlab algorithm was applied iteratively and the data except for the average deviation criterion removed from the original noisy data. In the second step, the WMA filter was applied in the time dimension to remove noise from the GPS observations containing displacements components. The purpose of removing the non-stationary noise component with low-frequency fluctuations is to obtain the stationary component including real displacement and random noise. Different filters were applied to clearly demonstrate the periodicities that occurred in the long- and short-time intervals; a low-pass filter (MA) for the low-frequency (long-term periodic) components and a differentiation filter (based on FIR) for high-frequency (short-term periodic) components. Low- and high-pass filters offer a good solution for the removal of dynamic and frequency modes of the structures. As an example of the former, an MA filter is suitable and simple to extract static and semi-static displacements of structures based on GPS tracking observation. The use of a high-pass filter also yielded favorable results in the extraction of dynamic displacement and frequency modes.

In step 3, the filtered signal was multiplied by a typical Hamming window function, which is generally used to prevent spectral leakage. In the fourth step, the sub-signal values of the signals filtered with low- and high-pass filters were calculated in the frequency domain using FFT. In the fifth step, the power spectrum of the signal was calculated. The calculated frequency spectrum demonstrated the long-term periods at low frequencies and short-term periods (vibrations, noise, etc.) at high frequencies. From this frequency spectrum, the 24-hour long-periodical movements and 6-second short-periodical movements of the tower were determined. The sum of repeated frequency values in the frequency spectrum presented the dominant frequencies. Since the high-frequency repetitive high-amplitude modes represented meaningful components in the signal, a model of the signal could be obtained with the selected mode values. Therefore, in the sixth step, with the reconstruction of the signals using IFFT with the first four mode values, position changes in the time domain were obtained. As a result, since the positional accuracy was limited to cm horizontally with the GPS technique, the positional change was modeled at the cm sensitivity level (Fig. 10).

The following important conclusions can be drawn from the examination of the frequency spectrum: the dominant frequency values were similar and the amplitude was

different in the x and y series. The data analyzed allowed observing the frequency spectrum in a region up to a duration of 72 hours. Since the motions examined were in the + and – direction, the greatest periodic motion was found at 36 hours, which was half the observation period. The dominant frequency value from the whole dataset showed a periodic motion of 24 hours. Finally, the analysis of the Endem TV tower in the time and frequency domains indicated safe oscillation expected under current loads.

The RTK-GPS method can provide significant displacement data in the time and frequency domains of building components. The results clearly showed that a series of long observations is needed to determine movement over a long time, and a high sampling rate is necessary for recording data at short time intervals to demonstrate repetitive movements. In measurements at a high sampling rate, the separation of short-time deviations does not disturb the overall course of the measurements. Long-time deviations of data result in the loss of positional information. Due to the long-term nature of the observations in this study, it is possible that the general movement of the structure was not detected.

This study aimed to determine the steps for the spectral analysis process and the displacement parameters of noisy RTK GPS data used in structural health monitoring. In this sense, this work presents a process of mathematical modeling in this area and provides a detailed visualization of the steps to be followed for the spectral analysis of GPS data.

References

- Blais, J.A.R. (1988), *Estimation and Spectral Analysis*, The University of Calgary Press, Calgary, Alberta, Canada.
- Box, G.E.P. and Jenkins, G.M. (1970), *Time-Series Analysis: Forecasting and Control*, Holden-Day, San Francisco, U.S.A.
- Bracewell, R.N. (2000), *The Fourier Transform and Its Applications*, 3rd Edition, McGraw-Hill, Stanford University, U.S.A.
- Brownjohn, J.M.W. (2005), "Lateral loading and response for a tall building in the non-seismic doldrums", *Eng. Struct.*, **27**(12), 1801-1812.
- Byrnes, J.S. and Byrnes, J.L. (1989), *Recent Advances in Fourier Analysis and Its Applications*, Kluwer Academic Publishers with NATO Scientific Affairs Division.
- Cooley, J.W. and Tukey, J.W. (1965), "An algorithm for machine calculation of complex fourier series", *Math. Comp.*, **19**, 297-301.
- Duran, A. and Earleywine, M. (2012), "GPS data filtration method for drive cycle analysis applications", *Proceedings of the SAE 2012 World Congress*, April.
- Elbeltagi, E., Kaloop, M.R. and Elnabwy, M.T. (2015), "GPS-monitoring and assessment of Mansoura railway steel-bridge based on filter and wavelet methods", *Asian J. Earth Sci.*, **8**(4), 114-126.
- Erdogan, H. and Gulal, E. (2009), "The application of time series analysis to describe the dynamic movements of suspension bridges", *Nonlin. Anal.: Real World Appl.*, **10**(2), 910-927.
- Floyd, M.A. (2017), *Time Series and Error Analysis*, Massachusetts Institute of Technology, Cambridge, MA, School of Earth Sciences, University of Bristol, U.K., May.
- Gikas, V. (2012), "Ambient vibration monitoring of slender structures by microwave interferometer remote sensing", *J.*

- Appl. Geodesy*, **6**, 167-176.
- Goudarzi, M.A., Cocard, M., Santerre, R. and Woldai, T. (2012), "GPS interactive time series analysis software", *GPS Solut.*, **17**(4), 595-603.
- Han, S. and Rizos, C. (1997), "Multipath effects on GPS in mine environments", *Proceedings of the Xth International Congress of the International Soc. Mine surveying*, Fremantle, Australia, November.
- Han, S. and Rizos, C. (2000), "GPS multipath mitigation using FIR filters", *Surv. Rev.*, **35**(277), 487-498.
- Herring, T.A., Melbourne, T.I., Murray, M.H., Floyd, M.A., Szeliga, W.M., King, R.W., Phillips, D.A., Puskas, C.M., Santillan, M. and Wang, L. (2016), "Plate boundary observatory and related networks: GPS data analysis methods and geodetic products", *Rev. Geophys.*, **54**(4), 759-808.
- Heslop, D. and Dekkers, M.J. (2002), "Spectral analysis of unevenly spaced climatic time series using CLEAN: Signal recovery and derivation of significance levels using a Monte Carlo simulation", *Phys. Earth Planet. Int.*, **130**(1-2), 103-116.
- Hristopoulos, D.T., Mertikas, S.P., Arhontakis, I. and Brownjohn, J.M.W. (2007), "Using GPS for monitoring tall-building response to wind loading: Filtering of abrupt changes and low-frequency noise, variography and spectral analysis of displacements", *GPS Solut.*, **11**(2), 85-95.
- James, J.F. (1995), *A Student's Guide to Fourier Transforms with Applications in Physics and Engineering*, Cambridge University Press.
- Kaloop, M.R. and Kim, D. (2014), "GPS-structural health monitoring of a long span bridge using neural network adaptive filter", *Surv. Rev.*, **46**(334), 7-14.
- Li, X., Ge, L., Ambikairajah, E., Rizos, C., Tamura, Y. and Yoshida, A. (2006), "Full-scale structural monitoring using an integrated GPS and accelerometer system", *GPS Solut.*, **10**(4), 233-247.
- Li, X., Ge, L., Peng, G.D., Rizos, C., Tamura, Y. and Yoshida, A. (2004), "Seismic response of a tower as measured by an integrated RTK-GPS system", *Proceedings of the 1st FIG International Symposium on Engineering Surveys for Construction Works and Structural Engineering*, University of Nottingham, U.K., June-July.
- Li, X. (2004), "The advantage of an integrated RTK-GPS system in monitoring structural deformation", *J. Glob. Position. Syst.*, **3**(1-2), 191-199.
- Mertikas, S.P. (1994), "The description of accuracy using conventional and robust estimates of scale", *Mar. Geod.*, **17**(4), 251-269.
- Moschas, F. and Stiros, S. (2013), "Noise characteristics of high-frequency, short-duration GPS records from analysis of identical, collocated instruments", *Measure.*, **46**(4), 1488-1506.
- Nikitopoulou, A., Protopsalti, K. and Stiros, S. (2006), "Monitoring dynamic and quasi-static deformations of large flexible engineering structures with GPS: Accuracy limitations and promises", *Eng. Struct.*, **28**(10), 1471-1482.
- Ogaja, C. and Satirapod, C. (2007), "Analysis of high-frequency multipath in 1-Hz GPS kinematic solutions", *GPS Solut. Spring. Verlag.*, **11**(4), 269-280.
- Oppenheim, A.V., Schaffer, R.W. and Buck, J.R. (1999), *Discrete-Time Signal Processing*, 2nd Edition, Upper Saddle River, Prentice Hall, New Jersey, U.S.A.
- Pehlivan, H., Aydin, O., Gulal, E. and Bilgili, E. (2013), "Determining the behavior of high-rise structures with geodetic hybrid sensors", *Geomat. Nat. Haz. Risk.*, **6**(8), 702-717.
- Pehlivan, H. and Bayata, H.F. (2016), "Usability of inclinometers as a complementary measurement tool in structural monitoring", *Struct. Eng. Mech.*, **58**(6), 1077-1085.
- Press, W.H., Flannery, B.P., Teukolsky, S.A. and Vetterling, W.T. (1992), *Numerical Recipes in Fortran*, 2nd Edition, The Art of Scientific Computing, 490ff, 551-556, 569-576, Cambridge University Press, New York, U.S.A.
- Roberts, G.W., Meng, X. and Dodson, A.H. (2004), "Integrating a global positioning system and accelerometers to monitor the deflection of bridges", *J. Surv. Eng.*, **130**(2), 65-72.
- Satirapod, C., Wang, J. and Rizos, C. (2001), "A new stochastic modelling procedure for precise static GPS positioning", *Zeitschrift für Vermessungswesen (ZfV)*, **126**, 356-372.
- Walker, J.S. (1996), *Fast Fourier Transformation*, 2nd Edition, CRC Press.
- Welsch, W. (1996), "Geodetic analysis of dynamic processes, Classification and Terminology", *Proceedings of the 8th International FIG-Symposium on Deformation Measurements*, Hong Kong.
- Xu, L., Guo, J. and Jiang, J.J. (2002), "Time frequency analysis of a suspension bridge based on GPS", *J. Sound Vibr.*, **254**(1), 105-116.
- Yan, H.M., Zhong, M. and Zhu, Y.Z. (2003), "The determination of degrees of freedom for digital filtered time series", *Acta Astronom. Sin.*, **44**(3), 324-329.
- Yi, T.H., Li, H.N. and Gu, M. (2011c), "A new method for optimal selection of sensor location on a high-rise building using simplified finite element model", *Struct. Eng. Mech.*, **37**(6), 671-684.
- Yi, T.H., Li, H.N. and Gu, M. (2013a), "Wavelet based multi-step filtering method for bridge health monitoring using GPS and accelerometer", *Smart Struct. Syst.*, **11**(4), 331-348.
- Yi, T.H., Li, H.N. and Gu, M. (2013b), "Experimental assessment of high-rate GPS receivers for deformation monitoring of bridge", *J. Int. Measure. Confederat.*, **46**(1), 420-432.
- Yi, T.H., Li, H.N. and Gu, M. (2011a), "Characterization and extraction of global positioning system multipath signals using improved particle filtering algorithm", *Measure. Sci. Technol.*, **22**(7), 075101.
- Yi, T.H., Li, H.N. and Gu, M. (2012), "Recent research and applications of GPS-based monitoring technology for high-rise structures", *Struct. Contr. Health. Monitor.*, **20**(5), 649-670.
- Yi, T.H., Li, H.N. and Gu, M. (2011b), "Optimal sensor placement for structural health monitoring based on multiple optimization strategies", *Struct. Des. Tall Spec. Build.*, **20**(7), 881-900.
- Yigit, C.O., Li, X., Inal, C., Ge, L. and Yetkin, M. (2010), "Preliminary evaluation of precise inclination sensor and GPS for monitoring full-scale dynamic response of a tall reinforced concrete building", *J. Appl. Geodesy.*, **4**(2), 103-113.
- Yigit, C.O. (2016), "Experimental assessment of post-processed kinematic precise point positioning method for structural health monitoring", *Geomat. Nat. Haz. Risk.*, **7**(1), 360-383.

CC